Multifunctionality of PAI-1 in fibrogenesis: Evidence from obstructive nephropathy in PAI-1–overexpressing mice[1]

Shunya Matsuo, Jesús M. López-Guisa, Xiaohe Cai, Daryl M. Okamura, Charles E. Alpers, Roger E. Bumgarner, Mette A. Peters, Guoqiang Zhang, and Allison A. Eddy

Children's Hospital and Regional Medical Center and Department of Pediatrics, Department of Pathology, and Department of Microbiology, University of Washington, Seattle, Washington

Multifunctionality of PAI-1 in fibrogenesis: Evidence from obstructive nephropathy in PAI-1–overexpressing mice.

Background. Plasminogen activator inhibitor-1 (PAI-1) has been implicated in the pathogenesis of chronic kidney disease based on its up-regulated expression and on the beneficial effects of PAI-1 inhibition or depletion in experimental models. PAI-1 is a multifunctional protein and the mechanisms that account for its profibrotic effects have not been fully elucidated.

Methods. The present study was designed to investigate PAI-1–dependent fibrogenic pathways by comparing the unilateral ureteral obstruction model (UUO) (days 3, 7, and 14) in *PAI-1*–overexpressing mice (*PAI-1* tg) to wild-type mice, both on a C57BL6 background.

Results. Following UUO, total kidney *PAI-1* mRNA and/or protein levels were significantly higher in the *PAI-1* tg mice ($N = 6$ to 8/group) and fibrosis severity was significantly worse (days 3, 7, and 14), measured both as Sirius red–positive interstitial area (e.g., $10 \pm 3.2\%$ vs. $4.5 \pm 1.0\%$) (day 14) and total kidney collagen (e.g., 11.1 ± 1.7 vs. 6.2 ± 1.3 µg/mg) (day 14). By day 14, the expression of two normal tubular proteins, E-cadherin and Ksp-cadherin, were significantly lower in the *PAI-1* tg mice ($3.2 \pm 0.5\%$ vs. $11.7 \pm 5.9\%$ and 2.6 ± 1.6) vs. $6.2 \pm 0.8\%$, respectively), implying more extensive tubular damage. At least four fibrogenic pathways were differentially expressed in the *PAI-1* tg mice. First, interstitial macrophage recruitment was more intense ($P < 0.05$ days 3 and 14). Second, interstitial myofibroblast density was greater ($P < 0.05$ days 3 and 7) despite similar numbers of proliferating tubulointerstitial cells. Third, transforming growth factor-β1 (TGF-β1) and collagen I mRNA were significantly higher. Finally, urokinase activity was significantly lower ($P < 0.05$ days 7 and 14) despite similar mRNA levels. Gene microarray studies documented that that the deletion of this single profibrotic gene had far-reaching consequences on renal cellular responses to chronic injury.

Conclusion. These data provide further evidence that PAI-1 is directly involved in interstitial fibrosis and tubular damage via two primary overlapping mechanisms: early effects on interstitial cell recruitment and late effects associated with decreased urokinase activity.

Despite many studies documenting the current worldwide epidemic of chronic kidney disease and the rapidly escalating costs of treating patients with end-stage kidney disease, advances in treatment have been rather modest. Recent investigations suggest that plasminogen activator inhibitor-1 (PAI-1) might be an effective therapeutic target [1]. Absent in normal kidneys, the response of both glomeruli and the tubulointerstitium to chronic injury is characterized by local PAI-1 production [2]. Evidence for a pathogenic role for PAI-1 in renal fibrogenesis comes from experimental studies that report less severe renal fibrosis and damage in PAI-1–deficient mice [3] and in mice treated with a mutant competitive PAI-1 inhibitor [4]. Although more controversial, humans expressing the 4G/4G polymorphic variant of the PAI-1 gene promoter express higher plasma PAI-1 levels and these individuals may be at increased risk for certain renal diseases such as diabetic nephropathy [5].

The process of renal interstitial fibrogenesis can be arbitrarily divided into four sequential and overlapping pathogenetic mechanisms: (*1*) acute renal damage that triggers a cellular phase characterized by inflammatory cell recruitment and later the appearance of myofibroblasts; (*2*) synthesis of profibrotic growth factors and cytokines primarily by these new interstitial cells but also by tubular cells; (*3*) excessive accumulation of extracellular matrix proteins as productions rates increase and/or protease-dependent degradation is inhibited; and (*4*) progressive nephron destruction as interstitial capillaries and tubules are obliterated [6, 7]. Initially, the profibrotic actions of PAI-1 seemed obvious. As a serine protease inhibitor, PAI-1 should impair the turnover and degradation of extracellular matrix proteins that accumulate at fibrotic sites by decreasing the activity of several relevant proteases: plasminogen activators, plasmin and metalloproteases. But recently it has become less clear

whether these proteases actually diminish fibrosis. When the gene encoding tissue-type plasminogen activator (tPA) was genetically deleted, matrix metalloprotease-9 (MMP-9) activity was also diminished but the tPA-null mice developed less severe fibrosis after ureteral obstruction than wild-type mice [8]. This rather surprising outcome was attributed to better preservation of tubular basement membranes and fewer interstitial myofibroblasts as a result of reduced epithelial-mesenchymal transition. Also of possible relevance is the ability of plasmin to activate latent transforming growth factor-β (TGF-β), at least in vitro. A recent experimental glomerulonephritis study in PAI-1–deficient mice reported worse glomerular damage and higher active TGF-β levels compared to wild-type mice [9] although a similar study reported reduced glomerular injury in PAI-1–deficient mice [10]. In our study of the unilateral ureteral obstruction (UUO) model, PAI-1 deficiency decreased fibrosis severity but significant differences in urokinase-type plasminogen activator (uPA) and plasmin activity could not be demonstrated [3]. A recent study by Edgtton et al [11] found that plasminogen deficiency failed to attenuate renal fibrosis in an obstructive uropathy model. Thus, it remains unclear to what extent PAI-1 promotes fibrosis via the inhibition of protease-dependent matrix degradation.

It is now recognized that PAI-1 exerts a powerful influence on cell migratory behavior that is dictated by the nature of the microenvironment within which it finds itself and might influence the earlier cellular phase of renal fibrogenesis [12–14]. Although the PAI-1 protease inhibitory domain may be involved, the critical effect involves interactions with vitronectin and the uPA receptor (uPAR) and at least one of several uPAR coreceptors [integrins, gp130, low-density lipoprotein (LDL) receptor-associated protein/α_2-macroglobulin, uPAR-associated protein/Endo180, and mannose-6-phosphate receptor/insulin-like growth factor type II (IGFII) receptor] [15]. While many in vitro studies suggest that PAI-1 inhibits cell migration, in vivo when PAI-1 is expressed in a more complex matrix environment, it generally promotes cell migration. This latter effect has been clearly shown in both animal models of and humans with various adenocarcinomas [16–18]. It was therefore of interest that the attenuation of renal fibrosis in PAI-1–deficient mice with obstructive uropathy was associated with an impressive delay in the recruitment of macrophages and myofibroblasts into the interstitium, suggesting important modulatory effects of PAI-1 on cellular behavior within the kidney [3].

In order to gain further insights into the profibrotic effects of PAI-1, the present study was designed to evaluate the consequences of PAI-1 overexpression on the renal responses to chronic injury induced by ureteral ligation.

METHODS

Experimental design

Studies were performed on male mice genetically engineered to overexpress PAI-1 (*PAI-1* tg) and wild-type C57BL/6 mice (*PAI-1* wild-type). Breeding pairs of the *PAI-1* tg mice on a C57BL/6 background that express a murine *PAI-1* minigene under the control of a cytomegalovirus (CMV) promoter were generously provided by Dr. D. Ginsburg, Howard Hughes Medical Institute, University of Michigan Medical Center, Ann Arbor, Michigan [19]. The wild-type C57BL/6 mice were purchased from Harlan Laboratories (Kent, WA, USA). The *PAI-1* genotype was confirmed by Northern blot measurements of hepatic and kidney mRNA levels. Both *PAI-1* tg and wild-type mice were randomly assigned into four groups: sham surgery, 3-day UUO, 7-day UUO, and 14-day UUO. These time points were selected as representative of the early phase when cellular recruitment is just beginning (day 3), a midpoint when growth factor–dependent matrix accumulation has begun (day 7) and a more advanced phase when irreversible kidney damage is evident (day 14). All surgeries were performed under general anesthesia at the age of 16 to 20 weeks. In the UUO group, the left ureter was exposed through a mid-abdominal incision and ligated using 4-0 silk. Sham-operated mice had their ureters exposed and manipulated without ligaton. 5-bromo-2′-deoxyuridine (BrdU) (Sigma Chemical Co., St. Louis, MO, USA) was injected intraperitoneally (50 µg/g body weight) 24 hours prior to the sacrifice to label proliferating cells. Animals were killed by exsangination under general anesthesia with isoflurane; the kidneys were harvested and the capsule removed. Livers were harvested from the 7-day UUO groups to confirm the genotype. Each kidney was weighed and cut into several pieces for RNA and protein extraction and histologic studies as previously described [20]. Frozen tissue samples were stored at −80°C. All procedures were performed in accordance with the guidelines established by National Research Council Guide for the Care and Use of Laboratory Animals.

Histologic examination

Picrosirius red staining. To evaluate the severity of interstitial fibrosis histologically, 3 µm sections of paraffin-embedded tissue were stained with the picrosirius red. Sections were deparaffinized by baking at 55°C for 1 hour, hydrated, and stained with picrosirius red solution (0.1% sirius red in saturated picric acid) for 18 hours, followed by treatment with 0.01 N HCl for 2 minutes, dehydration, and coverslip mounting. Sections were examined by polarized light microscopy. The image (×400 magnification) of five random, nonoverlapping cortical fields per each

slide were captured using a SPOT digital camera (Diagnostic Instruction, Inc., Sterling Heights, MI, USA), and the stained tubulointerstitial area was quantified using a computer-assisted image analysis system (Image-Pro Plus software) (Media Cybernetics, Silver Spring, MD, USA) as previously described [21]. Results were expressed as percentage of total tubulointerstitial area stained.

Immunostaining. Immunohistochemical staining was performed on paraffin-embedded sections or cryosections using procedures established in our laboratory using Vectastain *Elite* ABC Kits (Vector Laboratories, Inc., Burlingame, CA, US) and AEC Substrate Chromogen K3464 (Dako Corp., Carpinteria, CA, USA) as the peroxidase substrate. Horseradish peroxidase–conjugated, F(ab′)$_2$ goat antirat IgG (Accurate Chemical & Scientific Corp., Westbury, NY, USA) was used to detect primary rat monoclonal antibodies. Primary antibodies used were reactive with mouse PAI-1 (rabbit IgG ASMPAI-GF) (Molecular Innovations, Inc., Southfield, MI, USA), myofibroblasts (peroxidase-conjugated murine antihuman α-smooth muscle actin (α-SMA) 1A4 monoclonal antibody (Dako Corp.), macrophages (rat antimouse F4/80 monoclonal antibody) (Serotec, Ltd., Oxford, UK), and proliferating cells (MAS 250 rat anti-BrdU monoclonal antibody) (Harlan SeraLab, Ltd., Loughborough, UK), and goat antimouse E-cadherin (R&D Systems Inc., Minneapolis, MN, USA). Apoptotic cell nuclei were detected by terminal deoxynucleotidyl transferase(TdT)-mediated deoxyuridine triphosphate (dUTP) nick-end labeling (TUNEL) staining as previously described [22]. The number of positive cells was determined by manually counting at least four randomly selected cortical fields using a 10 mm × 10 mm grid as previously described [23].

Total collagen assay

To estimate total kidney collagen content, hydroxyproline was measured as previously described with minor modifications [3]. Each weighed kidney sample was hydrolyzed in 6 N HCl for 18 hours at 110°C and dried by speed vacuum centrifugation for 2 hours. Dried samples were solublized in citric acid buffer (0.23 mol/L citric acid, 0.88 mol/L sodium acetate trihydrate, 0.85 mol/L sodium hydroxide, and 1.2% acetic acid) and filtered through 0.45 μm centrifugal filter units (Ultrafree MC) (Millipore Co., Billerica, MA, USA). Samples diluted in citric acid buffer (20 μL) were loaded into each well of a microtiter plate, followed by 100 μL of chloramine T solution (1.4% chloramine T and 10% n-propanol in citric acid buffer). After a 15-minute incubation at room temperature, 100 μL of Erlich's solution (15% p-dimethylaminobenzaldehyde, 62% n-propanol, and 18% perchloric acid) was added and the mixture incubated for 20 minutes at 65°C. The optical density was read at 550 nm and the amount of hydroxyproline was determined against a standard curve

generated using known concentrations of hydroxyproline (Sigma Chemical Co.). Total collagen in the tissue was calculated on the assumption that collagen contains 12.7% hydroxyproline by weight. Final results were expressed as μg collagen/mg kidney wet weight.

Renal protease activity

Plasminogen gel zymography. Pieces of frozen kidney were homogenized in buffer [1% sodium dodecyl sulfate (SDS) in 50 mmol/L Tris, pH 7.6]. The protein concentration was determined using the BCA protein assay (Pierce Biotechnology, Rockford, IL, USA), and aliquots were stored at −80°C prior to analysis. Protein samples (10 μg) were separated by electrophoresis in 10% SDS-polyacrylamide gels containing plasminogen (10 μg/mL) and casein (2 mg/mL). The gels were washed with 2.5% Triton X-100 to remove SDS, and incubated for 16 hours at 37°C in a 0.1 mol/L glycine solution, and stained with Coomassie brilliant blue. The gel was photographed, and the size of each lytic band was measured using the image analysis software program. To distinguish PAs from metalloproteinases, the samples were also run on gel without plasminogen as previous described [3]. A human uPA standard (Calbiochem-Novabiochem Corp., La Jolla, CA, USA) was loaded into the outer lane.

Northern blotting

Total kidney RNA was extracted using the Trizol single-step reagent (Gibco BRL Life Technologies, Grand Island, NY, USA). Total kidney RNA (20 μg) from each individual animal was separated by electrophoresis in a 1.0% agarose formaldehyde gel, transferred to a nylon membrane (Nytran) (Schleicher & Schuell Bioscience, Inc., Keene, NH, USA) by capillary blotting, and fixed by ultraviolet cross-linking. The membranes were hybridized at 65°C for 16 hours in a solution containing cDNA probes radiolabeled with ^{32}P deoxycytidine triphosphate (dCTP) (BLU-513) (Perkin Elmer Life Sciences, Inc., Boston, MA, USA). Membranes were washed twice in 2 × standard sodium citrate (SSC) with 0.1% SDS at room temperature for 15 minutes, followed by one wash in 0.1 × SSC with 0.1% SDS at 55°C for 30 minutes. After washing, autoradiographs were obtained. The results were adjusted for RNA loading inequality based on the density of the ethidium bromide–stained 18s ribosomal bands as previously described [24]. cDNA probes used were rat PAI-1 from Dr. T. Gelehrter (University of Michigan, Ann Arbor, MI, USA) [25], rat α1(I) procollagen from Dr. S. Thorgeirsson (National Cancer Institute, Bethesda, MD, USA) [26], rat TGF-β1 from Dr. S. Qian (National Cancer Institute) [27], rat uPA from Dr. J. Degen (University of Cincinnati, OH, USA), mouse protease nexin-1 from Dr. D. Belin (University of Geneva, Switzerland) [28], and rat monocyte

chemoattractant protein-1 (MCP-1) from Dr. B. Rollins, (Dana-Farber Cancer Institute, Boston, MA, USA) [29].

Kidney gene microarray analysis

Total kidney RNA was isolated from five individual *PAI-1* wild-type mice and five *PAI-1* tg mice after 7 days of UUO using RNeasy Protect Mini kit (Qiagen, Inc., Valencia, CA, USA) according to the manufacturer's instructions. RNA quantity and quality were assessed by ultraviolet spectrophotometry (OD260/280). RNA quality was also determined using the Agilent Bioanalyzer 2100. Five micrograms total RNA was used for double-stranded cDNA synthesis by Affymetrix standard procedures for Eukaryotic target preparation. Synthesis of biotin-labeled cRNA was carried out by in vitro transcription using the Enzo BioArray High Yield RNA Transcript Labeling kit (Enzo Life Sciences, Inc., Farmingdale, NY, USA). Each biotin-labeled target was hybridized to Affymetrix Mouse U74Av2 arrays and processed according to standard Affymetrix procedures (*http://www. affymetrix.com/support/technical/manuals.affx*). Image processing was performed using Affymetrix MAS-5 software. The raw data were loaded into the Rosetta Resolver® Gene Expression Data Analysis System (Rosetta Biosoftware, Seattle, WA, USA) using standard methods. A *t* test analysis was used to identify genes differentially expressed between the two groups of five biologic replicates for each. A *P* value ≤ 0.01 was considered indicative of differential expression. Gene lists were analyzed and grouped based on Gene Ontology (GO) description of biologic process and molecular function as determined using the Affymetrix Gene Ontology Mining Tool at *https://www.affymetrix.com/analysis/*. These studies were done in collaboration the Center for Expression Arrays, University of Washington.

Western blotting

Kidney protein samples (20 μg), prepared as described for zymography, were separated by 10% SDS-polyacrylamide gel electrophresis (PAGE) and transferred to nitrocellulose membranes. The primary antibodies were sheep antimouse PAI-1 IgG (American Diagnostica Inc., Greenwich, CT, USA), mouse anti-Ksp-cadherin (Zymed Laboratories Inc., South San Francisco, CA, USA), goat antimouse E-cadherin (R&D Systems Inc.). The secondary antibodies were horseradish peroxidase–conjugated rabbit antisheep IgG (Santa Cruz Biotechnology, Inc., Santa Cruz, CA, USA), horseradish peroxidase–conjugated rabbit antimouse IgG, and horseradish peroxidase–conjugated rat antigoat IgG (Chemicon International, Inc., Temecula, CA, USA). Protein bands were visualized using the enhanced chemiluminescence (ECL) de-
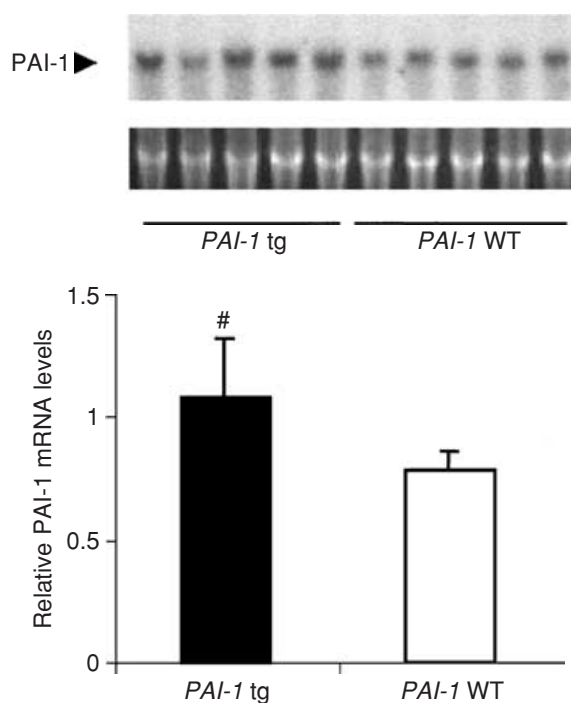

Fig. 1. Hepatic plaminogen activator inhibitor 1 (PAI-1) mRNA levels are higher in *PAI-1* tg mice. The upper autoradiograph is a Northern blot of hepatic PAI-1 RNA isolated from mice on day 7 unilateral ureteral obstruction (UUO). Shown below each lane is the corresponding ethidium bromide–stained 18s ribosome band. The graph represents the results of PAI-1 band density measurements expressed as mean fold increase ± 1 SD. #*P* < 0.05 compared with *PAI-1* wild-type (WT) group.

tection system (Pierce Biotechnology). Band intensities were measured using the Image-Pro Plus software and adjusted for protein loading equality as determined by Ponceau S staining.

Statistical analysis

All data are presented as the mean ± 1 SD. Results were analyzed by Mann-Whitney *U* test. A *P* value <0.05 was considered statistically significant.

RESULTS

PAI-1 genotyping

Hepatic *PAI-1* mRNA levels at 7 days' UUO, used as a confirmatory measure of the genotype, were significantly higher in *PAI-1* tg mice than in wild-type mice (Fig. 1).

Renal PAI-1 expression

Renal PAI-1 mRNA was induced in response to UUO. The mean mRNA levels were significantly higher (two- to threefold) in *PAI-1* tg mice compared to wild-type mice at each time point (Fig. 2). Kidney PAI-1 protein levels were higher in *PAI-1* tg mice compared with wild-type mice at each time point. By immunoblotting PAI-1 protein was detectable in *PAI*-1tg mice at 3 days, but it was
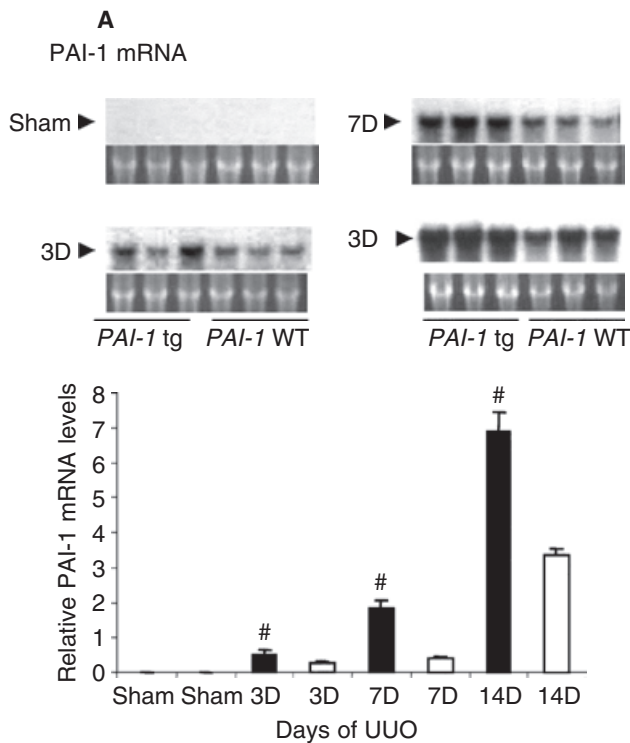
A

PAI-1 mRNA

Fig. 2. Kidney plasminogen activator inhibitor-1 (PAI-1) expression levels are higher in *PAI-1* tg mice after unilateral ureteral obstruction (UUO). (*A*) PAI-1 mRNA. A representative PAI-1 Northern blot autoradiograph illustrates renal mRNA levels with 28s ribosome bands below each lane. The graph summarizes the results of band density measurements ($N = 6$/group) expressed as mean fold increase ± 1 SD. #$P < 0.05$ compared with *PAI-1* wild-type (WT) group at the same time point. PAI-1 mRNA was not detectable in either sham group. (*B*) PAI-1 protein. A representative Western blot illustrates the 50 kD PAI-1 protein in *PAI-1* tg mice from 3 days onward, and in the wild-type mice beginning on day 7. The graph summarizes the results of band density measurements ($N = 6$/group) expressed as mean fold increase ± 1 SD. #$P < 0.05$ compared with *PAI-1* wild-type group at the same time point. By immunostaining PAI-1 protein was strongly expressed in renal tubules but also within the interstitium (day 14 shown). In general staining intensity was greater in the *PAI-1* tg mice (A) compared to *PAI-1* WT mice (B) (magnification ×400).

not identified in wild-type mice until 7 days (Fig. 2). By immunostaining, PAI-1 protein was detected in both renal tubules and the interstitium and was more intense in the PAI-1 tg mice (Fig. 2).

Severity of renal fibrosis

The total kidney collagen content was significantly increased in response to UUO in both genotypes but levels were significantly higher in *PAI-1* tg mice than in wild-type mice at 3 days, 7 days, and 14 days (Fig. 3). By sirius red staining, used to provide a histologic correlate to total kidney collagen, the percentage of the tubulointerstitium occupied by collagen was significantly greater in *PAI-1* tg mice at 7 days and 14 days (Fig. 4).
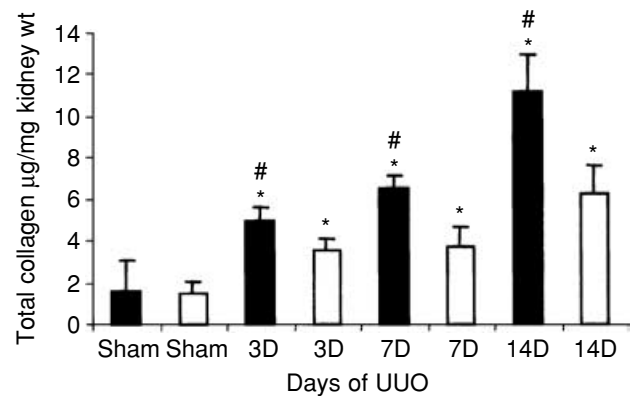

Fig. 3. Total kidney collagen levels are significantly higher in plasminogen activator inhibitor (*PAI-1*) tg mice. Results are expressed as mean ± 1 SD. The symbols are: (■) *PAI-1* tg mice; (□) *PAI-1* wild-type (WT) mice. #$P < 0.05$ compared to *PAI-1* WT group at the same time point; *$P < 0.05$ compared to sham group of same genotype.

Profile of intrarenal PAs

By plasminogen gel zymography, urokinase (uPA) activity was identified as a major ~ 40 kD lytic band and a smaller ~ 28 kD band and represented the predominant PA activity in kidney protein extracts. The tPA band was barely visible at all time points. The mean kidney uPA activity as evaluated by the size of each 40 kD band was increased in response to UUO in both genotypes (Fig. 5). Unlike the wild-type mice, the uPA activity was highest in the *PAI-1* tg mice at 3 days; by 14 days it was similar to activity levels in the sham *PAI-1* tg mice. The mean uPA activity was significantly lower in *PAI-1* tg mice at 7 days and 14 days than in wild-type mice. In contrast renal uPA mRNA levels increased in response to UUO but levels were similar between genotypes at all time points (Table 1).

From our previous UUO studies we had observed that the expression of protease nexin-1, another serine protease inhibitor that inhibits uPA, often increased in parallel with PAI-1 [abstract; Ikeda et al, J Am Soc Nephrol 12:722A, 2001]. In the present study it was also observed that protease nexin-1 mRNA levels increased in response to UUO and were significant higher in *PAI-1* tg mice than in wild-type mice at 3 days and 14 days (Table 1).

Interstitial inflammation

The renal response to UUO was characterized by the development of an interstitial infiltrate of monocytes/macrophages. The number of F4/80-positive interstitial macrophages was significantly higher in *PAI-1* tg mice than in wild-type mice at 3 days and 14 days (Fig. 6). Since MCP-1 has been identified in several studies as a significantly up-regulated chemokine in UUO [30], its expression was examined as a potential explanation for the difference in macrophage numbers. As expected, renal MCP-1 mRNA levels increased in response
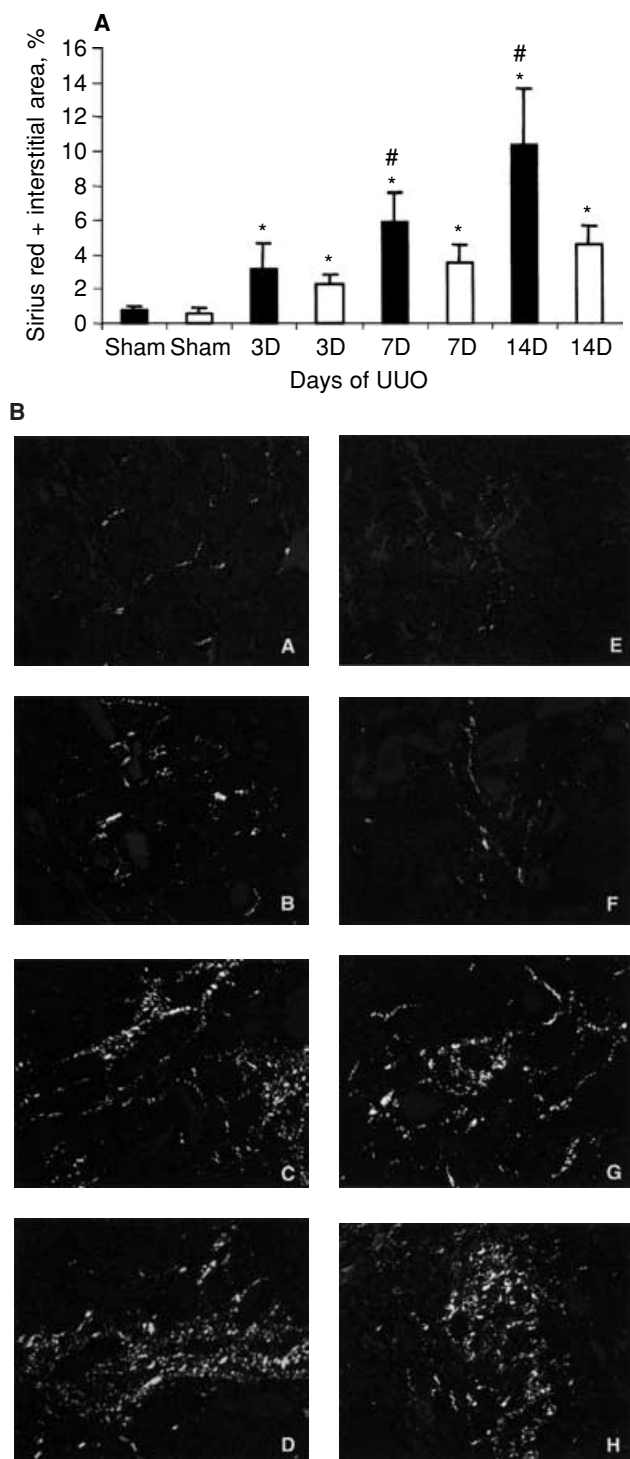
Fig. 4. Interstitial fibrosis severity is worse in plasminogen activator inhibitor (*PAI-1*) tg mice. (*A*) Graph illustrates the mean tubulointerstitial area occupied by collagen fibrils reactive with sirius red, expressed as mean% area ± 1 SD. The symbols are: (■) *PAI-1* tg mice; (□) *PAI-1* wild-type (WT) mice. #*P* < 0.05 compared with *PAI-1* wild-type group at the same time point; **P < 0.05 compared to sham group of same genotype. (*B*) Representative sirius red photomicrographs. Panels A to D are *PAI-1* tg mice that were sham-operated, and after 3, 7, and 14 days of unilateral ureteral obstruction (UUO), respectively. Panels E to H are *PAI-1* wild-type sham, 3, 7, and 14 days UUO, respectively (magnification 400×).

to UUO, but the mean levels were only higher in the *PAI-1* tg mice at 3 days (Table 1).

Interstitial myofibroblasts

α-SMA–positive myofibroblasts are considered the primary source of the interstitial matrix proteins that accumulate during fibrosis. The number of interstitial myofibroblasts increased in response to UUO; they appeared in significantly higher numbers in the *PAI-1* tg mice at 3 days and 7 days (Fig. 7). Proliferation of both tubular and interstitial cells was activated by UUO, peaking at 3 days (Table 2). However, the number of BrdU-positive tubulointerstitial cells was similar in mice of both genotypes, suggesting that differences in kidney cell proliferation rates do not account for the early differences in myofibroblast numbers. The number of apoptotic cells (mainly tubular) increased progressively after UUO, but the mean numbers were similar in the *PAI-1* tg and wild-type groups (Table 2).

Tubular epithelial cell damage

The cadherin family of proteins is a large group of calcium-dependent, membrane-associated molecules that are recognized as principal mediators of cell-cell adhesion. Loss of E-cadherin expression has been used as a marker of tubular epithelial-mesenchymal transition in many studies [31]. Ksp-cadherin is a 130 kD novel cadherin family member that is distinct from other cadherins in both structure and distribution as it is restricted to the basolateral membrane of kidney tubular epithelial cells. Loss of Ksp-cadherin expression has been used as a composite marker of tubular cell damage and atrophy [20]. By immunoblotting, E-cadherin protein levels after UUO but were significantly lower in the *PAI-1* tg mice at all time points (Fig. 8). Renal Ksp-cadherin expression decreased more rapidly in response to UUO in mice of both genotypes; levels were significantly lower in *PAI-1* tg mice than in wild-type mice at 14 days (Fig. 9).

TGF-β and procollagen genes

Given the significant early differences in interstitial cellularity in *PAI-1* tg, while serine protease activity was similar until the later time points, we examined the possibility that early differences in fibrosis severity might actually be due to enhanced matrix production. Impressive differences were detected, with mean renal TGF-β mRNA levels increased in response to UUO in both genotypes but to a significantly greater extent in the *PAI-1* tg mice at 3 days, 7 days, and 14 days (Fig. 10A). Renal procollagen α1(I) mRNA levels were also significantly higher in the *PAI-1* tg mice than in wild-type mice at 7 days and 14 days (Fig. 10B).
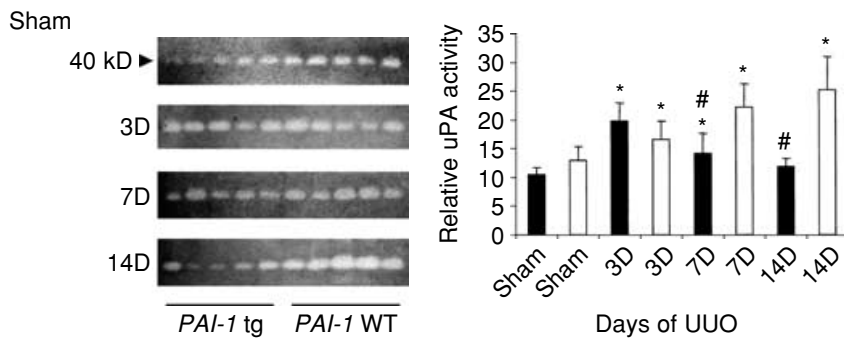
Fig. 5. Plasminogen gel zymogram demonstrates delayed effects of plasminogen activator inhibitor-1 (PAI-1) expression levels on renal urokinase-type plasmin activity (uPA). A representative zymogram illustrates plasminogen lytic activity of the 40 kD uPA protein. The graph shows the mean activity ± 1 SD. Symbols are: (■) *PAI-1* tg mice; (□) *PAI-1* wild-type (WT) mice. #$P < 0.05$ compared with *PAI-1* wild-type group at same time point; *$P < 0.05$ compared to sham group of same genotype.

Table 1. Urokinase-type plasminogen activator (uPA), protease nexin-1, and monocyte chemoattractant protein1-1 (MCP-1) relative mRNA levels

Gene	Sham		Day 3 UUO		Day 7 UUO		Day 14 UUO	
	PAI-1 tg	Wild-type	*PAI-1* tg	Wild-type	*PAI-1* tg	Wild-type	*PAI-1* tg	Wild-type
uPA	0.8 ± 0.4	1.0 ± 0.2	2.2 ± 0.2	2.0 ± 0.5	2.2 ± 0.3	1.8 ± 0.5	1.4 ± 0.6	1.4 ± 0.4
Nexin-1	1.0 ± 0.2	1.0 ± 0.1	11.0 ± 5.3[a]	4.6 ± 1.6	23.2 ± 3.4	20.0 ± 4.3	59.8 ± 5.9[a]	40.3 ± 1.7
MCP-1	0	0	2.0 ± 0.5	1.0 ± 0.6	2.7 ± 0.9	2.1 ± 0.8	3.9 ± 1.9	5.9 ± 1.6

Abbreviations are: UUO, unilateral ureteral obstruction; PAI-1, plasminogen activator inhibitor-1
[a]$P < 0.05$ compared with *PAI-1* wild-type group. Results are expressed as mean arbitrary densitometric units ± 1 standard deviation.

Differential gene expression profiles

Beyond regulating intrarenal serine protease activity, the results of this study indicated that overexpression of PAI-1 had a much broader impact on the fibrogenic response to sustained renal injury. To gain further insight into other pathways that might be directly or indirectly regulated by PAI-1, differential gene expression profiles were investigated 7 days after UUO using Affymetrix mouse U74Av2 GeneChip with 12,488 probes; 6268 with annotated biological function. A total of 261 genes with annotated biologic function were significantly increased and 203 were significantly decreased in the *PAI-1* tg mice. The differentially expressed genes and their associated GO biologic process, molecular function, and cellular component descriptions were manually scanned to select gene families most likely to be relevant to renal fibrosis and these are listed in Tables 3 and 4. Genes involved in metabolic pathways, electron transport, and transcription factors were in general not selected. Distinct genes encoding proteases/protease inhibitors, cell adhesion molecules, proinflammatory proteins, and proteins involved in cell proliferation and apoptosis were significantly up-regulated or down-regulated in the *PAI-1* tg mice compared to the *PAI-1* wild-type mice. Several cytoskeletal genes were up-regulated in the *PAI-1* tg mice while several heat shock and defense response genes and genes encoding transport proteins were significantly down-regulated in the *PAI-1* tg mice.

DISCUSSION

The results of this study add to the growing body of evidence that PAI-1 is a key mediator of progressive kidney
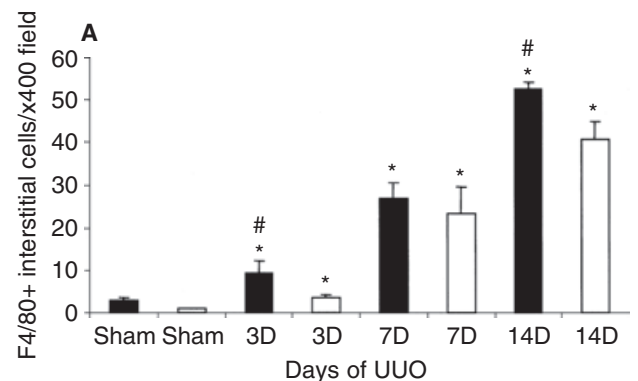

Fig. 6. Interstitial macrophage numbers are higher in plasminogen activator inhibitor-1 (*PAI-1*) tg mice. (*A*) The graph summarizes the number of F4/80-positive interstitial macrophages per 400× field expressed as mean number per field ± 1 SD. #$P < 0.05$ compared with *PAI-1* wild-type (WT) group at same time point; *$P < 0.05$ compared to sham group of same genotype. (*B*) Representative F4/80 immunohistochemical photomicrographs are *PAI-1* tg sham, 3, 7, and 14 days UUO, panels A to D, respectively, and *PAI-1* wild-type sham, 3, 7, and 14 days UUO, panels E to H, respectively (magnification ×400).

disease [2]. Genetically induced overexpression of PAI-1 resulted in a doubling of renal fibrosis severity compared to wild-type animals after 14 days of ureteral obstruction. Although measurement of renal functional differences is not possible in the UUO model, the major structural consequence of interstitial fibrosis that determines functional decline is tubular damage and destruction [7]. Tubular injury as evaluated by the loss of two normal tubular epithelial cell adhesion molecules, E-cadherin and Ksp-cadherin, was also significantly greater in PAI overexpressing mice after 14 days of UUO. The gene microarray
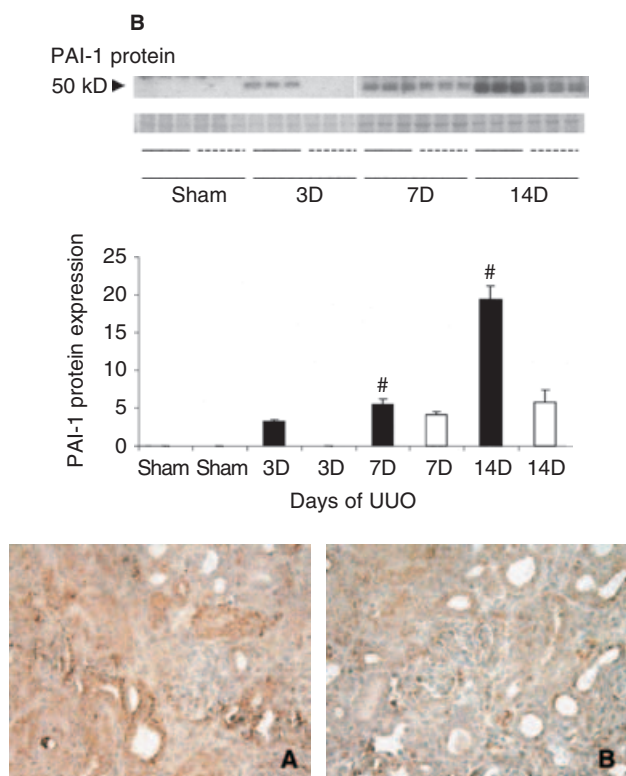
B

PAI-1 protein

50 kD ▶

Sham   3D   7D   14D

Fig. 2. (continued)

Fig. 6. (continued)

data identified several genes encoding transport proteins to be significantly decreased in the *PAI-1* tg mice, further evidence of more extensive tubular damage. Tubular cell death in progressive kidney disease is primarily due to apoptosis. Several proapoptotic genes (e.g., caspases 3, 4, and 7 and Bax) were significantly higher in the gene microarray analysis of the *PAI-1* tg mice and it has been suggested that PAI-1 may be involved in the activation of proapoptotic pathways [32]. However, just by counting the number of TUNEL+ apoptotic cells, we were unable to demonstrate significant PAI-1 genotype-dependent differences, perhaps because the critical time points were missed [33].

In addition to its well-defined role as a protease inhibitor, PAI-1 may also modulate several cellular functions via receptor-dependent interactions with the urokinase receptor (uPAR) and LDL receptor-related protein (LRP) [12–14]. The present study demonstrates a close association between interstitial cellularity and fibrosis severity, raising the possibility that one of the primary profibrotic effects of PAI-1 could be to facilitate interstitial inflammatory cell and myofibroblast recruitment. In general the intensity of interstitial inflammation correlates with the severity of damage in chronic kidney disease [34]. As a source of profibrotic growth factors such as TGF-β, macrophages are thought to ac-
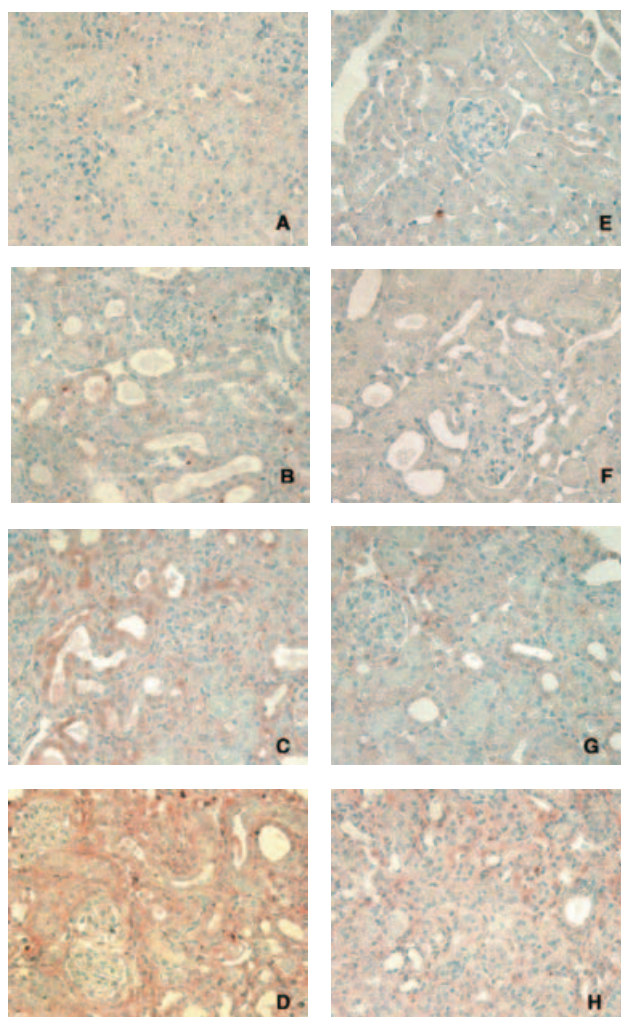
tively participate in renal fibrogenesis. In the present study, the more aggressive fibrogenic response in the PAI-1 tg mice was associated with worse interstitial inflammation. A similar association was observed in *PAI-1* tg mice with crescentic glomerulonephritis; both glomerular macrophage number and renal collagen content were significantly higher in the PAI-1 overexpressing mice [10]. PAI-1 might be functioning as a macrophage chemoattractant. We previously reported significantly less interstitial inflammation in PAI-1–deficient mice with UUO and proposed a potential macrophage chemotactic role for PAI-1 based on results of an in vitro chemotaxis study [3]. Recently Degryse et al [35] have reported that PAI-1 promotes smooth muscle cell chemotaxis via a pathway that involves LRP-dependent signaling. Since LRP is expressed by renal interstitial cells in obstructive uropathy [20], a similar PAI-1-LRP interaction might promote interstitial inflammation induced by chronic renal injury.
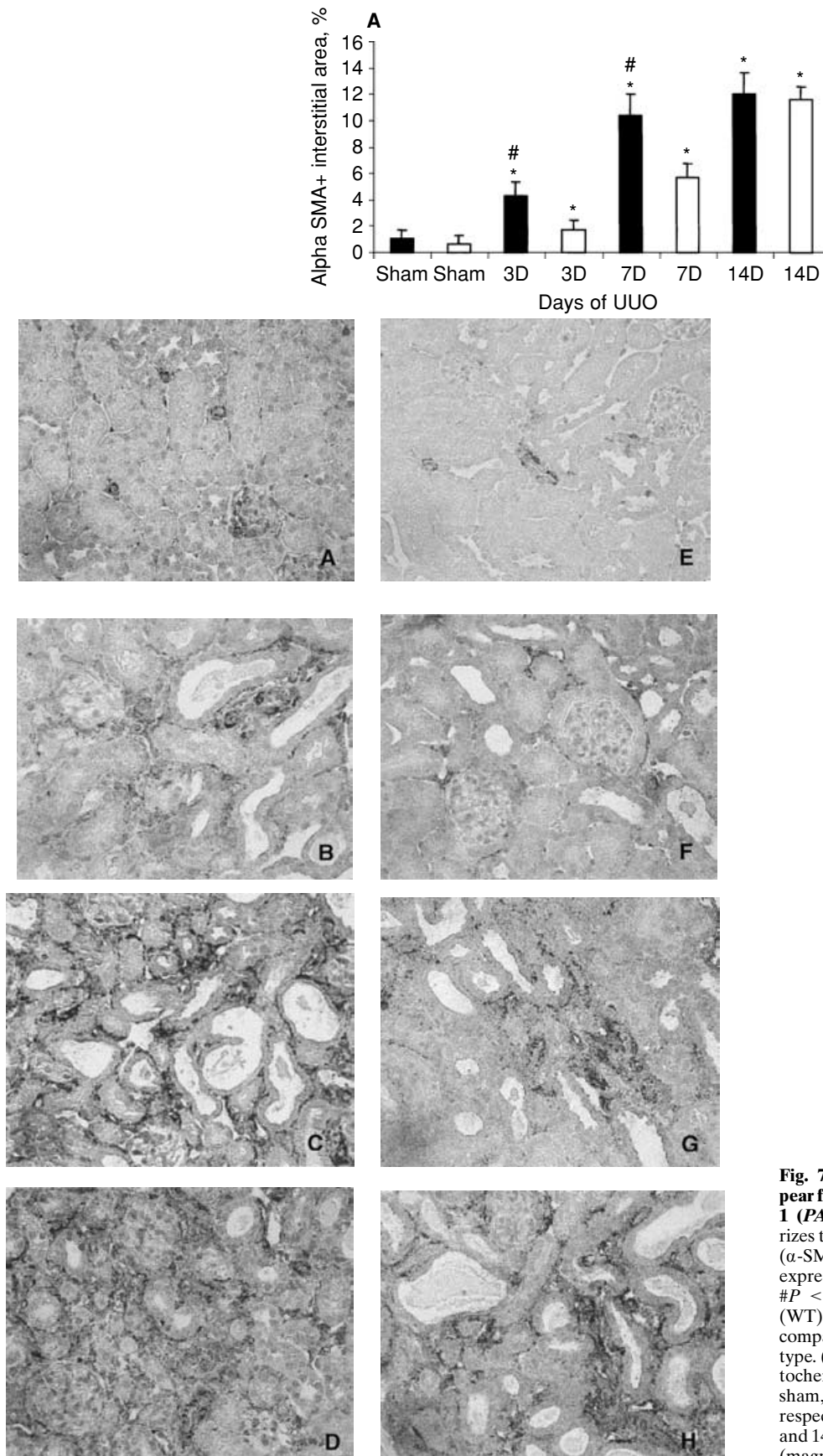
Fig. 7. Renal interstitial myofibroblasts appear faster in plasminogen activator inhibitor-1 (PAI-1) tg mice. (*A*) The graph summarizes the density of the α-smooth muscle actin (α-SMA)–positive interstitial myofibroblasts expressed as mean% positive area ± 1 SD. #*P* < 0.05 compared with *PAI-1* wild-type (WT) group at same time point; *P* < 0.05 compared to sham group of same genotype. (*B*) Representative α-SMA immunohistochemical photomicrographs are *PAI-1* tg sham, 3, 7, and 14 days UUO, panels A to D, respectively, and *PAI-1* wild-type sham, 3, 7, and 14 days UUO, panels E to H, respectively (magnification ×400).

Table 2. Proliferating and apoptotic tubulointerstitial cells

	Sham		Day 3 UUO		Day 7 UUO		Day 14 UUO	
	PAI-1 tg	Wild-type	*PAI-1* tg	Wild-type	*PAI-1* tg	Wild-type	*PAI-1* tg	Wild-type
BrdU+	3 ± 2	5 ± 2	88 ± 13	104 ± 17	33 ± 12	52 ± 9	40 ± 11	50 ± 17
TUNEL+	0.7 ± 0.7	1.0 ± 1.7	1.9 ± 1.1	1.4 ± 1.0	5.6 ± 2.3	6.1 ± 4.4	9.0 ± 5.6	7.7 ± 3.7

Abbreviations are: UUO, unilateral ureteral obstruction; PAI-1, plasminogen activator protein-1; BrdU, 5-bromo-2′-deoxyuridine; TUNEL, terminal deoxynucleotidyl transferase(TdT)-mediated deoxyuridine triphosphate (dUTP) nick-end labeling. Results are expressed as mean number of positive tubulointerstitial cells per 400× field ± 1 standard deviation.

Although plausible, it seems less likely that PAI-1 promotes monocyte migration indirectly via a coordinated up-regulation of chemokines or adhesion molecules. MCP mRNA levels were only significantly higher in the *PAI-1* tg mice 3 days after UUO. Gene microarray data on day 7 failed to identify other chemokines or leukocyte adhesion molecules as significantly up-regulated in *PAI-1* tg mice.

PAI-1 may also modulate cellular adhesion and migration via interactions between vitronectin, integrins, uPAR, and uPA [12–14]. This interplay is complex and highly dependent on the composition of the local environment but in general the high affinity of PAI-1 for vitronectin facilitates integrin-dependent ($\alpha v \beta 3$ in particular) cell migration whenever the extracellular environment contains alternative integrin ligands such as fibronectin. PAI-1 interacting with uPA-uPAR and αv integrins may also detach cells adherent to extracellular matrices and promote integrin-dependent clearance by endocytosis [36]. While the functional consequences of monocyte "detachment" within the kidney are open to speculation, it is tempting to suggest that directed migration to chemokines might be facilitated.

The extent to which the protease inhibitory actions of PAI-1 regulate the migration of inflammatory cells into the renal interstitium is currently unclear. Urokinase is the predominant serine protease in the renal tubulointerstitial compartment and the present as well as earlier studies have reported increased uPA mRNA expression and activity levels in the UUO model [3]. By cleaving its receptor to release soluble uPAR, urokinase may promote monocyte recruitment, as soluble uPAR interacts with the chemoattraction receptor FPRL1/LXA4 [37]. In vivo, mice lacking uPAR have significantly lower renal uPA activity and fewer interstitial macrophages than wild-type mice after ureteral obstruction [22]. Despite similar uPA mRNA levels in the *PAI-1* tg and wild-type mice, renal uPA activity was significantly lower in the PAI-1–overexpressing mice but not until day 7. Therefore, uPA-dependent chemotaxis does not explain the early differences in interstitial macrophage numbers.

Interstitial macrophages may contribute directly to progressive kidney disease via several mechanisms, the most important possibly being the synthesis of fibrogenic growth factors [34]. In support of this paradigm, the *PAI-1* tg mice with worse tubulointerstitial disease had significantly higher renal TGF-β mRNA levels on days 3 and 14 after UUO, paralleling the significant differences in interstitial macrophage numbers. Data derived from microarray analysis of differential gene expression identified several other cytokines and growth factor receptors that were significantly increased in the *PAI-1*-tg mice [including receptors for interleukin-4 (IL-4), tumor necrosis factor (TNF), fibroblast growth factor (FGF), activin, leukemia inhibitory factor, and retinoic acid]. The enhanced expression of these receptors might simply be attributed to the greater number of macrophages in the *PAI-1* tg mice or alternatively it may be these intrarenal macrophages are phenotypically and functionally distinct from macrophages in the kidneys of the wild-type mice— differences that might further contribute to accelerated fibrosis in the *PAI-1*-tg mice.

The second interstitial cell that is a critical mediator of progressive kidney disease is the myofibroblast. As in our previous study in PAI-1–deficient mice, PAI-1 expression levels had a significant impact on the rate of recruitment of interstitial myofibroblasts. Both 3 and 7 days after UUO, there were twice as many interstitial myofibroblasts in *PAI-1*-tg mice. After this early phase of injury, the number of interstitial myofibroblasts in the wild-type mice caught up to the *PAI-1* tg mice. Although the origin of renal interstitial myofibroblasts is still unclear, current evidence supports four distinct possibilities and the findings in this study suggest that PAI-1 may be directly involved in one or more of them. First, myofibroblasts may be recruited from circulating precursor cells although the contribution of this pathway appears to be modest [38–40]. Second, normal α-SMA–expressing perivascular cells might migrate into the interstitium under the influence of appropriate signals [41]. It is possible that like its effects on monocytes, PAI-1 facilitates the recruitment of interstitial myofibroblast precursor cells from the circulation or perivascular locations.

Third, resident interstitial fibroblasts may transform into myofibroblasts upon activation. Even though the proliferative rate of resident interstitial fibroblasts may be relatively low in response to damage, this pathway
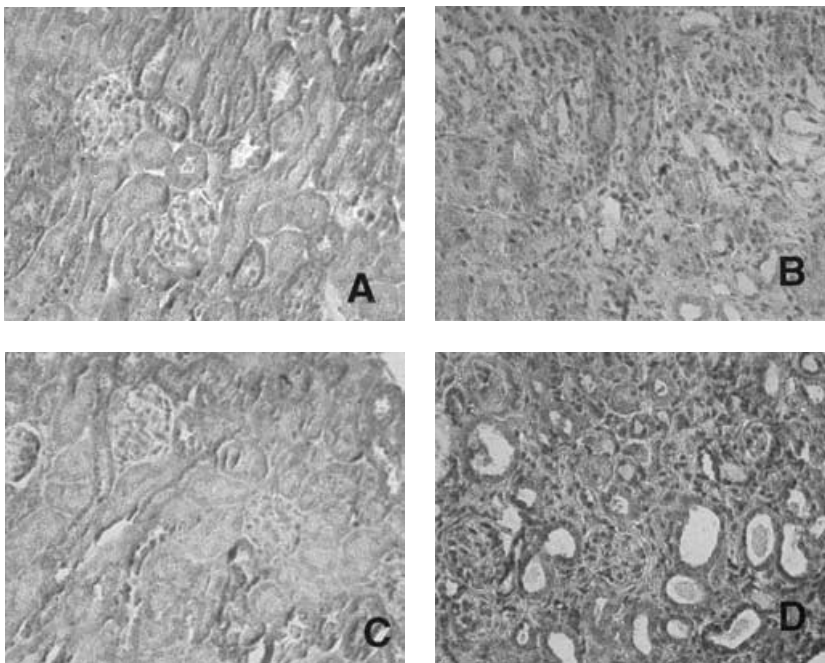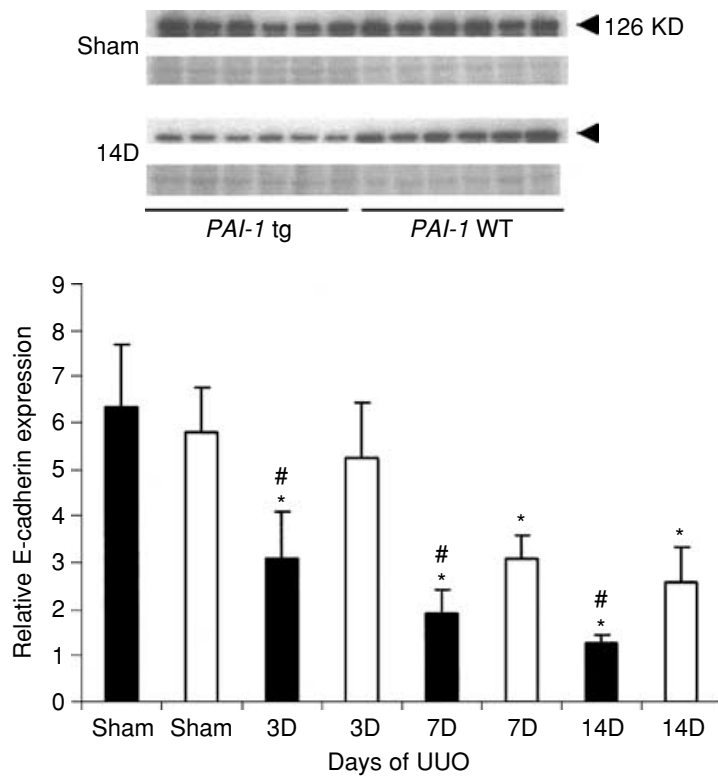
Fig. 8. Renal loss of E-cadherin occurs more rapidly in plasminogen activator inhibitor-1 (*PAI-1*) tg mice. The upper Western blot illustrates the changes in E-cadherin protein levels (126 kD) on 14 days' unilateral ureteral obstruction (UUO). Ponceau S staining shown below demonstrates the equivalency of protein loading and transfer. The graph summarizes the results of single band density measurements ($N = 6$/group/time point) expressed as mean fold increase ± 1 SD. Symbols are: (■) *PAI-1* tg mice; (□) *PAI-1* wild-type (WT) mice. #$P < 0.05$ compared with *PAI-1* wild-type group at same time point; *$P < 0.05$ compared with sham group of same genotype. Below, light photomicrographs of E-cadherin immunostaining are *PAI-1* tg mice (*A*) and *PAI-1* wild-type mice (*C*) in sham-operated group and *PAI-1* tg mice (*B*) and *PAI-1* wild-type mice (*D*) from the 14 days' UUO group (magnification ×400).

may contribute substantially to the myofibroblast population given their long half-life [24, 42, 43]. In the present study, most of the cells that proliferated after UUO were tubular cells. The numbers of BrdU-positive tubulointerstitial cells were similar in both genotypes suggesting that PAI-1 alone does not modulate fibroblast

proliferative rates, even though several genes involved in proliferation were differentially expressed between the *PAI-1* tg and the *PAI-1* wild-type mice.

The final pathway of myofibroblast recruitment is epithelial-mesenchymal transition (EMT). At least three key events are involved in the EMT process that leads
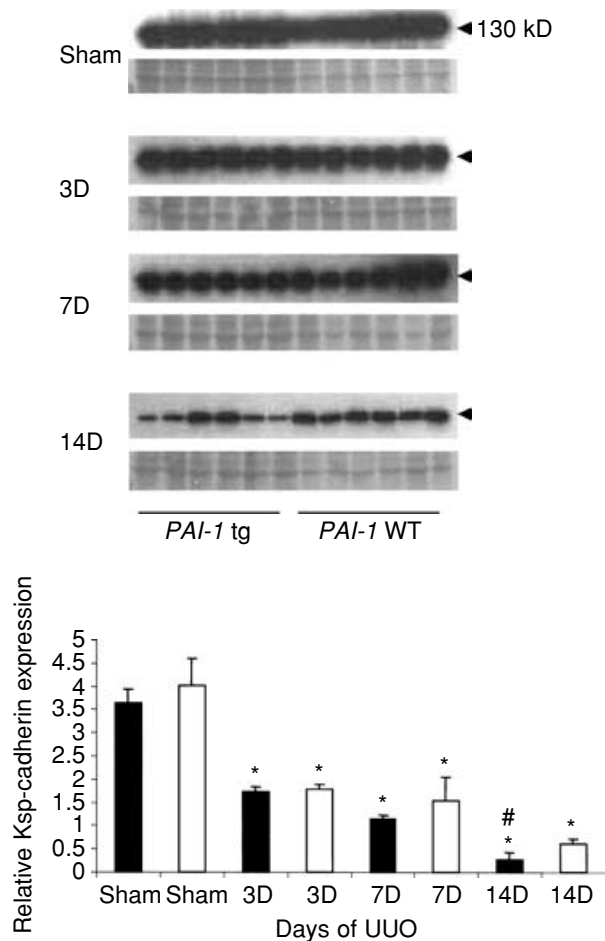
Fig. 9. Renal loss of Ksp-cadherin occurs more rapidly in plasminogen activator inhibitor (*PAI-1*) tg mice. The upper Western blots demonstrate a time-dependent alteration in Ksp-cadherin (130 kD) expression. Ponceau S staining shown in the lower portion illustrates the equivalency of protein loading and transfer. The graph summarizes the results of single band density measurements expressed as mean fold increase ± 1 SD. Symbols are: (■) *PAI-1 tg* mice; (□) *PAI-1* wild-type (WT) mice. #*P* < 0.05 compared with *PAI-1* wild-type group at same time point; *P* < 0.05 compared with sham group of same genotype.

to the appearance of these cells in the interstitium [31]. First, tubular epithelial cells must undergo phenotypic transformation, an event that is often identified experimentally by the loss of tubular cell adhesion molecules such as E-cadherin and the de novo expression of fibroblast proteins such as FSP-1 and α-SMA. In response to UUO, tubular cells produce PAI-1 and the rate of E-cadherin loss was significantly greater in the *PAI-1* tg mice. Whether PAI-1 plays a direct role in the phenotypic transformation of tubular epithelial cells or whether the acceleration of this change in the *PAI-1* tg mice is a consequence of the more aggressive inflammatory and fibrogenic responses cannot be determined by the present study. A direct tubular effect of PAI-1 would require the existence of a currently unknown PAI-1 receptor. Whether interactions with uPAR/uPA and basolateral
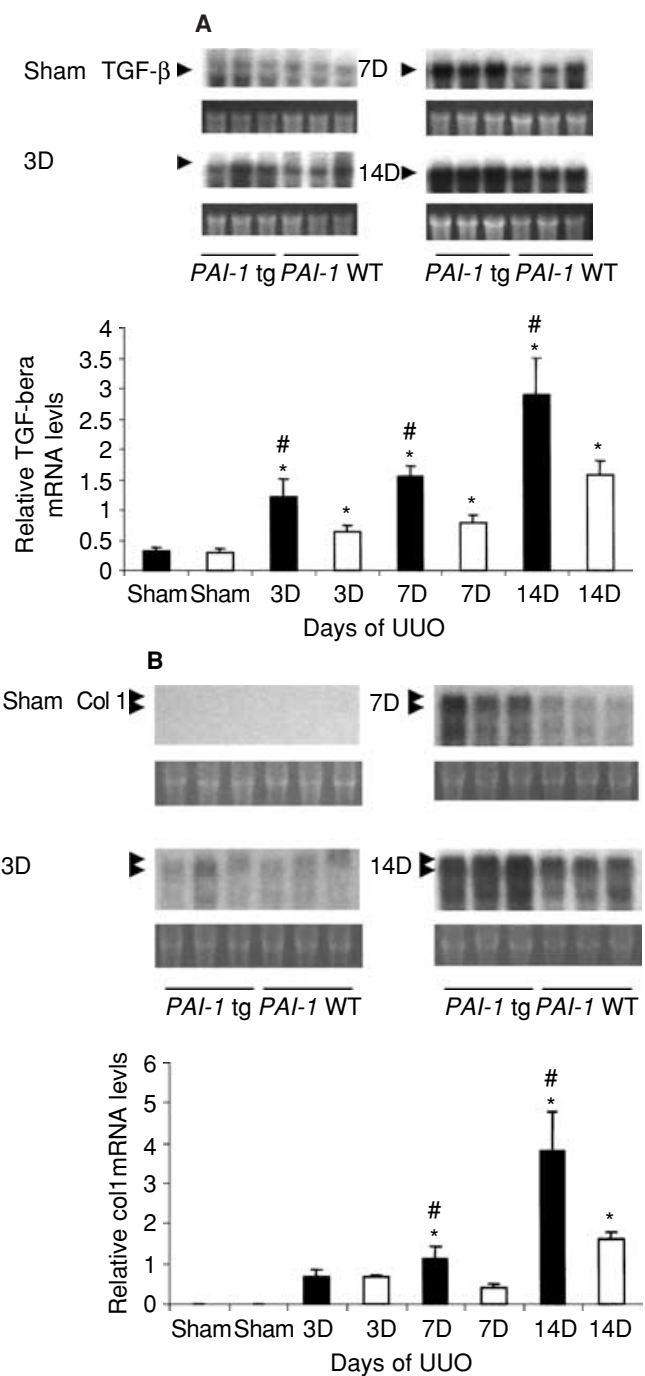

Fig. 10. Renal transforming growth factor-β (TGF-β) and α1(I) procollagen mRNA levels are higher in plasminogen activator inhibitor (*PAI-1*) tg mice. The autoradiographs of TGF-β (*A*) and α1(I) procollagen (*B*) are the Northern blots with 18s ribosome bands shows below each lane. The graphs summarize the results of each band density measurements (*N* = 6) expressed as mean fold increase ± 1 SD. #*P* < 0.05 compared with *PAI-1* wild-type (WT) group at same time point; *P* < 0.05 compared with sham group of same genotype.

LRP-1 or apical LRP-2 (megalin) could serve such a role deserves further consideration [44].

The second step requires disruption of the barrier between tubular cells and the interstitium that is imposed

Table 3. Genes significantly increased in plasminogen activator inhibitor-1 (PAI-1) *tg* mice

Proteases/inhibitors	
Serine (or cysteine) proteinase inhibitor, clade A, member 1b	*Serpina1b*
Serine (or cysteine) proteinase inhibitor, clade A, member 1a	*Serpina1a*
Alanyl (membrane) aminopeptidase	*Anpep*
Calpain 1	*Capn1*
Calpain 5	*Capn5*
Cathepsin F	*Ctsf*
Procollagen C-proteinase enhancer protein	*Pcolce*
Prolyl endopeptidase	*Prep*
Cathepsin B	*Ctsb*
Cytokines/growth factors	
Insulin-like growth factor binding protein, acid labile subunit	*Igfals*
Interleukin-4 receptor, alpha	*Il4ra*
Tumor necrosis factor receptor superfamily, member 1b	*Tnfrsf1b*
Milk fat globule-epidermal growth factor 8 protein	*Mfge8*
Fibroblast growth factor receptor 1	*Fgfr1*
Activin A receptor, type II-like 1	*Acvrl1*
Activin receptor IIB	*Acvr2b*
Insulin-like growth factor binding protein 1	*Igfbp1*
Leukemia inhibitory factor receptor	*Lifr*
Cell adhesion/communication	
Ninjurin 1	*Ninj1*
Flotillin 2	*Flot2*
SH3 domain protein 4	*Sh3d4*
Junction plakoglobin	*Jup*
Integrin beta$_5$	*Itgb5*
Gap junction membrane channel protein beta 2	*Gjb2*
Ras homolog gene family, member A	*Arha*
Carboxypeptidase $\times$ 2 (M14 family)	*Cpxm2*
Inflammation/immune response	
Scavenger receptor class B, member 1	*Scarb1*
Lymphocyte antigen 6 complex, locus E	*Ly6e*
TAP binding protein	*Tapbp*
Ia-associated invariant chain	*Ii*
Histocompatibility 2, class II, locus Mb1	*H2-DMb1*
Histocompatibility 2, class II antigen E beta	*H2-Eb1*
Histocompatibility 2, class II, locus DMa	*H2-DMa*
Proteasome (prosome, macropain) 28 subunit, alpha	*Psme1*
Lymphotoxin B	*Ltb*
Protein tyrosine phosphatase, nonreceptor type substrate 1	*Ptpns1*
Proliferation	
Par-6 (partitioning defective 6,) homolog alpha (*C. elegans*)	*Pard6a*
Bridging integrator 1	*Bin1*
Nuclear factor of activated T cells, cytoplasmic 1	*Nfatc1*
Neuroblastoma, suppression of tumorigenicity 1	*Nbl1*
Schlafen 2	*Slfn2*
Cell division cycle 37 homolog (*S. cerevisiae*)	*Cdc37*
Growth arrest and DNA-damage-inducible 45 beta	*Gadd45b*
Mitogen activated protein kinase kinase 7	*Map2k7*
Midkine	*Mdk*
v-crk sarcoma virus CT10 oncogene homolog (avian)-like	*Crkl*
Thymoma viral proto-oncogene 2	*Akt2*
v-erb-b2 erythroblastic leukemia viral oncogene homolog 3 (avian)	*Erbb3*
Stratifin	*Sfn*
v-maf musculoaponeurotic fibrosarcoma oncogene family, protein F (avian)	*Maff*
Jun-B oncogene	*Junb*
Block of proliferation 1	*Bop1*
Apoptosis	
Bcl2-associated X protein (BAX)	*Bax*
Lymphocyte-specific 1	*Lsp1*
Caspase 3, apoptosis-related cysteine protease	*Casp3*
Defender against cell death 1	*Dad1*
Caspase 4, apoptosis-related cysteine protease	*Casp4*
Caspase 7	*Casp7*
Cytoskeleton	
Actin-related protein 2/3 complex, subunit 1A	*Arpc1a*
Paralemmin	*Palm*
Par-6 (partitioning defective 6) homolog alpha (*C. elegans*)	*Pard6a*
Microtubule-associated protein tau	*Mapt*
Tubulin, alpha 6	*Tuba6*

Table 3. Continued.

Tubulin, alpha 1	*Tuba1*
Erythrocyte protein band 4.1	*Epb4.1*
Synaptogyrin 1	*Synaptogyrin 1*
Cofilin 1, nonmuscle	*Cfl1*
Development	
LIM domain binding 1	*Ldb1*
Sema domain, immunoglobulin domain (Ig), short basic domain, secreted, (semaphorin) 3B	*Sema3b*
Sema domain, immunoglobulin domain (Ig), transmembrane domain (TM) and short cytoplasmic domain, (semaphorin) 4A	*Sema4a*
Ephrin B1	*Efnb1*
Male-enhanced antigen 1	*Mea1*
Dickkopf homolog 3 (*Xenopus laevis*)	*Dkk3*
Frizzled homolog 1 (*Drosophila*)	*Fzd1*
COP9 (constitutive photomorphogenic) homolog, subunit 3 (*Arabidopsis thaliana*)	*Cops3*
Homeo box D10	*Hoxd10*
Homeo box A11	*Hoxa11*
Retinoic acid receptor, alpha	*Rara*
Stimulated by retinoic acid gene 6	*Stra6*
Miscellaneous	
Peroxisome proliferators-activated receptor alpha	*Ppara*
Amyloid beta (A4) precursor protein-binding, family A, member 3	*Apba3*
Leukotriene C4 synthase	*Ltc4s*
Peroxiredoxin 2	*Prdx2*
Angiotensinogen	*Agt*
Retinoic acid receptor, gamma	*Rarg*
Growth arrest specific 6	*Gas6*

by the tubular basement membrane. Mediated by matrix-degrading proteases, it is easy to envisage how PAI-1 might block rather than promote tubular basement membrane damage since the activity of PAs, plasmin and plasmin-activated metalloproteinases should, if anything, be decreased in the presence of excessive PAI-1. During the third step, transdifferentiated tubular cells migrate into the interstitium. Little is currently known about the signals that control this migration but PAI-1 could potentially have a modulatory role.

One of the more surprising findings in the present and other recent studies is the lack of compelling in vivo evidence that the profibrotic effects of PAI-1 are tightly associated with its inhibitory effects on proteases. Renal urokinase activity was significantly lower in the *PAI-1* tg mice on days 7 and 14 while the differences in inflammation and fibrosis began much earlier, on day 3. It is possible that the assays were not sufficiently sensitive to detect early differences, but it is also plausible that the protease-dependent effects of PAI-1 are less prominent, especially during the initial phase of chronic injury. PAs are thought to be particularly important in fibrotic responses that are associated with fibrin provisional matrices such as occurs in the lung, although surprisingly, genetic fibrinogen deficiency does not alter the severity of pulmonary fibrosis in mice treated with bleomycin [45, 46]. In the kidney tPA but not uPA deficiency exacerbates the severity of crescentic glomerulonephritis associated with fibrin deposition [47]. In contrast, tPA deficiency actually attenuates the severity of renal fibrosis induced by UUO

possibly due to reduced MMP-9 activity, better preservation of tubular basement membranes and as a consequence, a reduction in the size of the interstitial myofibroblast population [8]. Direct antifibrotic actions for uPA appear more compelling based on experiments using urokinase therapy in models of pulmonary and hepatic fibrosis although data from renal models of progressive tubulointerstitial disease are not yet available [48–50]. The role of plasmin in fibrosis is complicated by the fact that it may either promote fibrosis by activating latent TGF-β or it may counteract fibrosis by activating latent metalloproteinases. Recent work based on studies of obstructive uropathy in plasminogen-deficient mice from our own and another laboratory suggest that the net in vivo effect of plasmin in the kidney is the enhancement of fibrosis (Zhang et al, manuscript in preparation) [11].

Does PAI-1 promote renal fibrosis by inhibiting matrix turnover? The present study cannot answer this question. The accelerated inflammation and myofibroblast recruitment associated with higher TGF-β and procollagen I mRNA levels indicate that matrix production rates were likely higher in *PAI-1* tg mice but delayed degradation due to lower uPA activity remains plausible. Another genotype-dependent difference was identified that could contribute to impaired matrix turnover in *PAI-1* tg mice. Given our earlier observation that the serine protease inhibitor protease nexin-1 and PAI-1 might be coregulated [abstract; Ikeda et al, *J Am Soc Nephrol* 12:722A, 2001], its expression was examined in the present study and

Table 4. Genes significantly decreased in plasminogen activator inhibitor-1 (PAI-1) tg mice

Proteases/inhibitors	
Tissue inhibitor of metalloproteinase 3	*Timp3*
Annexin A3	*Anxa3*
Serine (or cysteine) proteinase inhibitor, clade I, member 1	*Serpini1*
Serine protease inhibitor, Kazal type 3	*Spink3*
Phosphate-regulating gene with homologies to endopeptidases on the X chromosome	*Phex*
Cytokines	
Interferon-related developmental regulator 1	*Ifrd1*
S100 calcium binding protein A11 (calizzarin)	*S100a11*
Serine/threonine kinase receptor associated protein	*Strap*
Insulin-like growth factor 1	*Igf1*
Platelet derived growth factor, alpha	*Pdgfa*
Insulin-like growth factor binding protein 5	*Igfbp5*
Suppressor of cytokine signaling 2	*Socs2*
Cell adhesion	
Laminin B1 subunit 1	*Lamb1-1*
Vascular cell adhesion molecule 1	*Vcam1*
Nidogen 1	*Nid1*
Cadherin 11	*Cdh11*
Thrombospondin 1	*Thbs1*
Calcium and integrin binding 1 (calmyrin)	*Cib1*
Secreted phosphoprotein 1	*Spp1*
Tight junction protein 1	*Tjp1*
CEA-related cell adhesion molecule 9	*Ceacam9*
Integrin beta 1 (fibronectin receptor beta)	*Itgb1*
Proliferation	
Septin 2	*2-Sep*
Centrin 3	*Cetn3*
Checkpoint kinase 1 homolog (*S. pombe*)	*Chek1*
Topoisomerase (DNA) II beta	*Top2b*
RAD21 homolog (S. pombe)	*Rad21*
Origin recognition complex, subunit 4-like (*S. cerevisiae*)	*Orc4l*
Nuclear factor I/B	*Nfib*
Thioredoxin-like	*Txnl*
Protein phosphatase 3, catalytic subunit, alpha isoform	*Ppp3ca*
Cyclin G1	*Ccng1*
Phospholipase C, beta 1	*Plcb1*
Ribosomal protein S4, X-linked	*Rps4x*
Myelocytomatosis oncogene	*Myc*
Apoptosis	
Programmed cell death 6	*Pdcd6*
Tial1 cytotoxic granule-associated RNA binding protein-like 1	*Tial1*
Cytotoxic granule-associated RNA binding protein 1	*Tia1*
Growth arrest specific 2	*Gas2*
Carboxypeptidase E	*Cpe*
A disintegrin and metalloproteinase domain 9 (meltrin gamma)	*Adam9*
A disintegrin-like and metalloprotease (reprolysin type) with thrombospondin type 1 motif, 1	*Adamts1*
Proliferation-associated 2G4	*Pa2g4*
Proprotein convertase subtilisin/kexin type 5	*Pcsk5*
Glutamyl aminopeptidase	*Enpep*
Heat response	
Heat-responsive protein 12	*Hrsp12*
Heat shock protein 1 (chaperonin 10)	*Hspe1*
Heat shock protein 8	*Hspa8*
Heat shock 70 kD protein 5 (glucose-regulated protein)	*Hspa5*
Heat shock protein 1A	*Hspa1a*
Heat shock protein 105	*Hsp105*
Defense responses	
CD24a antigen	*Cd24a*
Periplakin	*Ppl*
Beta-2 microglobulin	*B_2m*
Histocompatibility 2, D region locus 1	*H2-D1*
Catalase	*Cat*
Immunoglobulin kappa chain variable 1 (V1)	*Igk-V1*
Immunoglobulin heavy chain (J558 family)	*Igh-VJ558*
Immunoglobulin heavy chain (V7183 family)	*Igh-V7183*
Immunoglobulin joining chain	*Igj*
T-cell cytokine receptor	*Tccr*

Table 4. Continued.

Complement	
Complement component factor h-like 1	*Cfhl1*
Complement component factor h	*Cfh*
Adipocyte complement-related protein	*Acrp30*
Transport	
ATPase, H+ transporting, V1 subunit B, isoform 2	*Atp6v1b2*
ATPase, H+ transporting, V1 subunit C, isoform 1	*Atp6v1c1*
Voltage-dependent anion channel 3	*Vdac3*
Chloride channel calcium activated 1	*Clca1*
Chloride channel 4 - 2	*Clcn4 - 2*
Folate receptor 2 (fetal)	*Folr2*
Albumin 1	*Alb1*
Hippocampus abundant gene transcript 1	*Hiat1*
Fatty acid binding protein 4, adipocyte	*Fabp4*
Solute carrier family 7 (cationic amino acid transporter, y+ system), member 10	*Slc7a10*
SMC2 structural maintenance of chromosomes 2-like 1 (yeast)	*Smc2l1*
Adaptor-related protein complex 3, sigma 1 subunit	*Ap3s1*
Cystic fibrosis transmembrane conductance regulator homologue	*Cftr*
Purinergic receptor P2X, ligand-gated ion channel, 1	*P2rx1*
Potassium voltage-gated channel, shaker-related subfamily, member 1	*Kcna1*
Solute carrier family 12, member 2	*Slc12a2*
Solute carrier family 35 (CMP-sialic acid transporter), member 1	*Slc35a1*
Miscellaneous	
Immediate early response 5	*Ier5*
Kidney androgen regulated protein	*Kap*
Cd63 antigen	*Cd63*
Neuroepithelial cell transforming gene 1	*Net1*
Growth hormone	*Gh*
Progesterone receptor membrane component 1	*Pgrmc1*
Mannose receptor, C type 1	*Mrc1*
Intelectin	*Itln*
Disabled homologue 1 (*Drosophila*)	*Dab1*
Ephrin B3	*Efnb3*
Dishevelled, dsh homologue 1 (*Drosophila*)	*Dvl1*
Tuftelin 1	*Tuft1*
von Hippel-Lindau binding protein 1	*Vbp1*
Endothelin 1	*Edn1*
ras homolog gene family, member B	*Arhb*

found to be significantly higher at 3 and 14 days. Protease nexin-1 inhibits uPA, plasmin, and thrombin, and it has been implicated in dysregulated matrix turnover associated with such disease processes as malignancy, glomerulonephritis and scleroderma [51–53]. The gene microarray data identified additional proteases and protease inhibitors that were differentially expressed between the genotypes that could potentially impact matrix remodeling and degradation.

CONCLUSION

The present study in PAI-1–overexpressing mice adds to the growing body of evidence that it has a very impressive fibrosis-promoting role. First recognized as a protease inhibitor, it is becoming increasingly clear that PAI-1 also plays an important role in the interstitial recruitment of inflammatory macrophages and myofibroblasts, especially during the early response to chronic injury. Our data suggest that these cellular effects are fundamental to the role of PAI-1 as a fibrogenic molecule. As the fibrogenic response progresses, modulatory ef-

fects on uPA activity are present that may further enhance matrix accumulation by impairing its turnover. Data from gene microarray studies demonstrate how the overexpression of this single profibrotic molecule has far-reaching effects on the renal molecular response to chronic damage. These data suggest that PAI-1 should be an excellent therapeutic target for chronic kidney disease prevention.

REFERENCES

1. INGELFINGER JR: Forestalling fibrosis. *N Engl J Med* 349:2265–2266, 2003
2. EDDY AA: Plasminogen activator inhibitor-1 and the kidney. *Am J Physiol Renal Physiol* 283:F209–F220, 2002
3. ODA T, JUNG YO, KIM H, et al: PAI-1 deficiency attenuates the fibrogenic response to ureteral obstruction. *Kidney Int* 30:587–596, 2001
4. HUANG Y, HARAGUCHI M, LAWRENCE DA, et al: A mutant, non-inhibitory plasminogen activator inhibitor type 1 decreases matrix accumulation in experimental glomerulonephritis. *J Clin Invest* 112:379–388, 2003
5. WONG TY, POON P, SZETO CC, et al: Association of plasminogen activator inhibitor-1 4G/4G genotype and type 2 diabetic nephropathy in Chinese patients. *Kidney Int* 57:632–638, 2000
6. EDDY AA: Molecular insights into renal interstitial fibrosis. *J Am Soc Nephrol* 7:2495–2508, 1996
7. EDDY AA: Molecular basis of renal fibrosis. *Pediatr Nephrol* 15:290–301, 2000
8. YANG J, SHULTZ RW, MARS WM, et al: Disruption of tissue-type plasminogen activator gene in mice reduces renal interstitial fibrosis in obstructive nephropathy. *J Clin Invest* 110:1525–1538, 2002
9. HERTIG A, BERROU J, ALLORY Y, et al: Type 1 plasminogen activator inhibitor deficiency aggravates the course of experimental glomerulonephritis through overactivation of transforming growth factor beta. *FASEB J* 17:1904–1906, 2003
10. KITCHING A, KONG Y, HUANG X, et al: Plasminogen activator deficiency-1 is a significant determinant of renal injury in experimental glomerulonephritis. *J Am Soc Nephrol* 2003 (in press)
11. EDGTTON KL, GOW RM, KELLY DJ, et al: Plasmin is not protective in experimental renal interstitial fibrosis. *Kidney Int* 66:68–76, 2004
12. OSSOWSKI L, AGUIRRE-GHISO JA: Urokinase receptor and integrin partnership: Coordination of signaling for cell adhesion, migration and growth. *Curr Opin Cell Biol* 12:613–620, 2000
13. KJOLLER L: The urokinase plasminogen activator receptor in the regulation of the actin cytoskeleton and cell motility. *Biol Chem* 383:5–19, 2002
14. BLASI F, CARMELIET P: uPAR: A versatile signalling orchestrator. *Nat Rev Mol Cell Biol* 3:932–943, 2002
15. PREISSNER KT, KANSE SM, MAY AE: Urokinase receptor: A molecular organizer in cellular communication. *Curr Opin Cell Biol* 12:621–628, 2000
16. BAJOU K, NOEL A, GERARD RD, et al: Absence of host plasminogen activator inhibitor 1 prevents cancer invasion and vascularization. *Nat Med* 4:923–928, 1998
17. DUFFY MJ: The urokinase plasminogen activator system: Role in malignancy. *Curr Pharm Des* 10:39–49, 2004
18. SIDENIUS N, BLASI F: The urokinase plasminogen activator system in cancer: Recent advances and implication for prognosis and therapy. *Cancer Metastasis Rev* 22:205–222, 2003
19. EITZMAN DT, MCCOY RD, ZHENG X, et al: Bleomycin-induced pulmonary fibrosis in transgenic mice that either lack or overexpress the murine plasminogen activator inhibitor-1 gene. *J Clin Invest* 97:232–237, 1996
20. ZHANG G, KIM H, CAI X, et al: Urokinase receptor deficiency accelerates fibrosis in obstructive nephropathy. *J Am Soc Nephrol* 14:1254–1271, 2003
21. KIM H, ODA T, LOPEZ-GUISA J, et al: TIMP-1 deficiency does not attenuate interstitial fibrosis in obstructive nephropathy. *J Am Soc Nephrol* 12:736–748, 2001
22. ZHANG G, KIM H, CAI X, et al: Urokinase receptor modulates cellular and angiogenic responses in obstructive uropathy. *J Am Soc Nephrol* 14:1254–1271, 2003
23. EDDY AA, MICHAEL AF: Acute tubulointerstitial nephritis associated with aminonucleoside nephrosis. *Kidney Int* 33:14–23, 1988
24. JONES CL, BUCH S, POST M, et al: The pathogenesis of interstitial fibrosis in chronic purine aminonucleoside nephrosis. *Kidney Int* 40:1020–1031, 1991
25. ZEHAB R, GELEHRTER TD: Cloning and sequencing of cDNA for the rat plasminogen activator inhibitor-1. *Gene* 73:459–468, 1988
26. NAKATSUKASA H, NAGY P, EVARTS RP, et al: Cellular distribution of

27. QIAN SW, KONDAIAH P, ROBERTS AB, et al: cDNA cloning by PCR of rat transforming growth factor β-1. *Nucl Acids Res* 18:3059, 1990
28. VASSALLI JD, HUARTE J, BOSCO D, et al: Protease-nexin 1 as an androgen-dependent secretory product of the murine seminal vesicle. *EMBO J* 12:1871–1878, 1993
29. ROLLINS BJ, MORRISON ED, STILES CD: Cloning and expression of JE, a gene inducible by platelet-derived growth factor and whose product has cytokine-like properties. *Proc Natl Acad Sci USA* 85:3738–3742, 1988
30. KITAGAWA K, WADA T, FURUICHI K, et al: Blockade of CCR2 ameliorates progressive fibrosis in kidney. *Am J Pathol* 165:237–246, 2004
31. LIU Y: Epithelial to mesenchymal transition in renal fibrogenesis: Pathologic significance, molecular mechanism, and therapeutic intervention. *J Am Soc Nephrol* 15:1–12, 2004
32. AL-FAKHRI N, CHAVAKIS T, SCHMIDT-WOLL T, et al: Induction of apoptosis in vascular cells by plasminogen activator inhibitor-1 and high molecular weight kininogen correlates with their anti-adhesive properties. *Biol Chem* 384:423–435, 2003
33. TRUONG LD, CHOI YJ, TSAO CC, et al: Renal cell apoptosis in chronic obstructive uropathy: The roles of caspases. *Kidney Int* 60:924–934, 2001
34. EDDY AA: Proteinuria and interstitial injury. *Nephrol Dial Transplant* 19:277–281, 2004
35. DEGRYSE B, NEELS JG, CZEKAY RP, et al: The low density lipoprotein receptor-related protein is a motogenic receptor for plasminogen activator inhibitor-1. *J Biol Chem* 279:22595–22604, 2004
36. CZEKAY RP, AERTGEERTS K, CURRIDEN SA, et al: Plasminogen activator inhibitor-1 detaches cells from extracellular matrices by inactivating integrins. *J Cell Biol* 160:781–791, 2003
37. RESNATI M, PALLAVICINI I, WANG JM, et al: The fibrinolytic receptor for urokinase activates the G protein-coupled chemotactic receptor FPRL1/LXA4R. *Proc Natl Acad Sci USA* 99:1359–1364, 2002
38. GRIMM PC, NICKERSON P, JEFFERY J, et al: Neointimal and tubulointerstitial infiltration by recipient mesenchymal cells in chronic renal-allograft rejection. *N Engl J Med* 345:93–97, 2001
39. IWANO M, PLIETH D, DANOFF TM, et al: Evidence that fibroblasts derive from epithelium during tissue fibrosis. *J Clin Invest* 110:341–350, 2002
40. HASHIMOTO N, JIN H, LIU T, et al: Bone marrow-derived progenitor cells in pulmonary fibrosis. *J Clin Invest* 113:243–252, 2004
41. RONNOV-JESSEN L, PETERSEN OW, KOTELIANSKY VE, et al: The origin of the myofibroblasts in breast cancer. Recapitulation of tumor environment in culture unravels diversity and implicates converted fibroblasts and recruited smooth muscle cells. *J Clin Invest* 95:859–873, 1995
42. MASAKI T, FOTI R, HILL PA, et al: Activation of the ERK pathway precedes tubular proliferation in the obstructed rat kidney. *Kidney Int* 63:1256–1264, 2003
43. TANG WW, ULICH TR, LACEY DL, et al: Platelet-derived growth factor-BB induces renal tubulointerstitial myofibroblast formation and tubulointerstitial fibrosis. *Am J Pathol* 148:1169–1180, 1996
44. MARZOLO MP, YUSEFF MI, RETAMAL C, et al: Differential distribution of low-density lipoprotein-receptor-related protein (LRP) and megalin in polarized epithelial cells is determined by their cytoplasmic domains. *Traffic* 4:273–288, 2003
45. HATTORI N, DEGEN JL, SISSON TH, et al: Bleomycin-induced pulmonary fibrosis in fibrinogen-null mice. *J Clin Invest* 106:1341–1350, 2000
46. PLOPLIS VA, WILBERDING J, MCLENNAN L, et al: A total fibrinogen deficiency is compatible with the development of pulmonary fibrosis in mice. *Am J Pathol* 157:703–708, 2000
47. KITCHING AR, HOLDSWORTH SR, PLOPLIS VA, et al: Plasminogen and plasminogen activators protect against renal injury in crescentic glomerulonephritis. *J Exp Med* 185:963–968, 1997
48. SISSON TH, HATTORI N, XU Y, et al: Treatment of bleomycin-induced pulmonary fibrosis by transfer of urokinase-type plasminogen activator genes. *Hum Gene Ther* 10:2315–2323, 1999

49. Salgado S, Garcia J, Vera J, *et al*: Liver cirrhosis is reverted by urokinase-type plasminogen activator gene therapy. *Mol Ther* 2:545–551, 2000
50. Hattori N, Mizuno S, Yoshida Y, *et al*: The plasminogen activation system reduces fibrosis in the lung by a hepatocyte growth factor-dependent mechanism. *Am J Pathol* 164:1091–1098, 2004
51. Moll S, Schaeren-Wiemers N, Wohlwend A, *et al*: Protease nexin 1 in the murine kidney: Glomerular localization and up-regulation in glomerulopathies. *Kidney Int* 50:1936–1945, 1996
52. Strehlow D, Jelaska A, Strehlow K, *et al*: A potential role for protease nexin 1 overexpression in the pathogenesis of scleroderma. *J Clin Invest* 103:1179–1190, 1999
53. Buchholz M, Biebl A, Neebetae A, *et al*: SERPINE2 (protease nexin I) promotes extracellular matrix production and local invasion of pancreatic tumors in vivo. *Cancer Res* 63:4945–4951, 2003